

Technical Notes

TECHNICAL NOTES are short manuscripts describing new developments or important results of a preliminary nature. These Notes should not exceed 2500 words (where a figure or table counts as 200 words). Following informal review by the Editors, they may be published within a few months of the date of receipt. Style requirements are the same as for regular contributions (see inside back cover).

Effects of Surface Tension on Two-Dimensional Two-Phase Stratified Flows

Y. F. Yap,* J. C. Chai,† T. N. Wong,‡ and K. C. Toh§
Nanyang Technological University,
Singapore 639798, Republic of Singapore

I. Introduction

SURFACE tension plays an important role in the evolution of the interface between two phases by smoothing sharp interfaces and minimizing the interfacial area. This in turn affects the flowfield of both phases. Therefore, an understanding of the effect of surface tension on low Reynolds number two-phase flow is essential.

One difficulty in simulating two-phase flows is due to the presence of an interface in the domain. Several methods are available to model the interface. These include but are not limited to the level-set (LSET) method,¹ the volume-of-fluid (VOF) method,² and the front-tracking method.³ In these methods, the effect of surface tension can be modeled using the continuum surface force (CSF) model⁴ as a concentrated force at the interface. Because the surface tension force is proportional to the interface curvature, accurate evaluation of the interface curvature is essential. Among the aforementioned methods, the LSET method offers a convenient way to calculate the curvature.

In this Note, the effect of surface tension on the interface evolution of a steady, two-dimensional, stratified two-phase flow is investigated using the LSET method. The surface tension force is modeled using the CSF approach. Localized mass correction (LMC)⁵ scheme is utilized to ensure mass conservation at every cross section.

II. Mathematical Formulation

A stratified flow of two immiscible fluids, as shown in Fig. 1, is considered. When a combined formulation is used, the continuity and momentum equations can be written as

$$\frac{\partial(\rho u_j)}{\partial x_j} = 0 \quad (1)$$

$$\begin{aligned} \rho u_j \frac{\partial u_i}{\partial x_j} = & \frac{\partial}{\partial x_j} \left(\mu \frac{\partial u_i}{\partial x_j} \right) - \frac{\partial p}{\partial x_i} + \frac{\partial}{\partial x_j} \left(\mu \frac{\partial u_j}{\partial x_i} \right) \\ & + \rho g_i + D(\xi) \sigma \kappa n_i \end{aligned} \quad (2)$$

The additional surface tension force [the last term of Eq. (2)] is modeled using the CFS method. Here κ and $D(\xi)$ are the curvature and the Dirac delta function, respectively. The density ρ and viscosity μ are calculated using

$$\alpha = (1 - H) \alpha_1 + H \alpha_2 \quad (3)$$

where the smoothed Heaviside function H is given by⁶

$$H = \begin{cases} 0 & \xi < -\varepsilon \\ [(\xi + \varepsilon)/2\varepsilon] + (1/2\pi) \sin(\pi\xi/\varepsilon) & |\xi| \leq \varepsilon \\ 1 & \xi > \varepsilon \end{cases} \quad (4)$$

The Heaviside function is smoothed over a finite thickness of ε . The parameter ε is related to the grid size and is normally taken as a factor of the grid spacing. In this Note, a uniform mesh (with $\Delta x = \Delta y$) is used. Numerical tests show that setting ε to Δx , $1.5\Delta x$, and $2\Delta x$ result in the same solution. As a result, ε is set to be the width of one control volume.

The LSET function ξ is defined as the signed distance function from the interface. The evolution of ξ is governed by

$$u_j \frac{\partial \xi}{\partial x_j} = 0 \quad (5)$$

To ensure that ξ remains a distance function for all time, redistancing is performed. This is achieved by solving for the steady-state solution of a second distance function ψ given by

$$\frac{\partial \psi}{\partial t} = \text{sign}(\xi)(1 - |\nabla \psi|) \quad (6)$$

The initial condition is $\psi(\mathbf{x}, 0) = \xi(\mathbf{x})$. The LMC⁵ procedure is used to ensure mass conservation. The steady-state solution to a third distance function ψ' is obtained using

$$\frac{\partial \psi'}{\partial t'} = \text{sign}(\xi_{\text{ref}}) \frac{(\dot{m}_d - \dot{m}_c)}{\dot{m}_d} \quad (7)$$

where \dot{m}_c and \dot{m}_d are the current and desired mass flow rates, respectively. The steady-state values of the second distance function

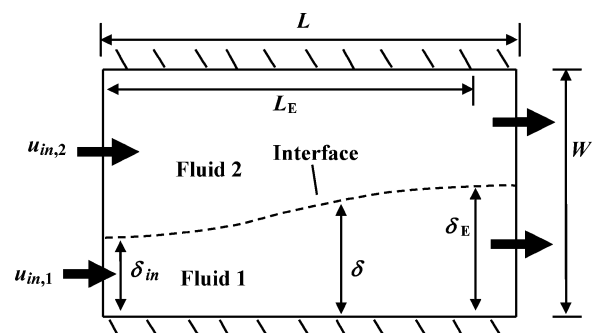


Fig. 1 Stratified two-phase flow between parallel plates.

Received 6 June 2005; revision received 22 November 2005; accepted for publication 31 December 2005. Copyright © 2006 by the American Institute of Aeronautics and Astronautics, Inc. All rights reserved. Copies of this paper may be made for personal or internal use, on condition that the copier pay the \$10.00 per-copy fee to the Copyright Clearance Center, Inc., 222 Rosewood Drive, Danvers, MA 01923; include the code 0887-8722/06 \$10.00 in correspondence with the CCC.

*Ph.D. Candidate, School of Mechanical and Aerospace Engineering, Nanyang Avenue.

†Associate Professor, School of Mechanical and Aerospace Engineering, Nanyang Avenue; mckchai@ntu.edu.sg. Senior Member AIAA.

‡Associate Professor, School of Mechanical and Aerospace Engineering, Nanyang Avenue.

§Associate Professor, School of Mechanical and Aerospace Engineering, Nanyang Avenue.

ψ are used as the initial condition for Eq. (7). Either fluid can be used as the reference fluid for the LMC procedure.

The velocity at the inlet is specified. No-slip condition is applied at the wall. At the outlet, zero gradient of the velocity is imposed. The LSET function is specified at the inlet. At the wall and the outlet, the zero gradient condition is used for the LSET function. Details of the solution procedure are given in Ref. 5 and will not be repeated here.

III. Results and Discussion

Figure 1 shows the schematic of a stratified two-phase flow between two parallel plates. Two immiscible fluids flow a distance L between two parallel plates separated by a height W . At the inlet, the interface is located at δ_{in} . The development of the velocity profiles in the developing region causes the interface δ between the two fluids to evolve. Once the fully developed region is reached, the velocity profile and the interface location δ_E become independent of the axial coordinate.

For given ρ_1/ρ_2 , μ_1/μ_2 , \dot{V}_1/\dot{V}_2 , and δ_{in}/W combination, three additional dimensionless parameters, namely, the Reynolds number $Re = \rho_2 u_m W / \mu_2$, the capillary number $Ca = u_m \mu_2 / \sigma$, and the Eotvos number $Eo = |\rho_1 - \rho_2| g W^2 / \sigma$, are required to characterize the flow.

Here ρ_1/ρ_2 , μ_1/μ_2 , \dot{V}_1/\dot{V}_2 , and Reynolds number Re are set to 2.0, 2.0, $\frac{3}{2}$, and 0.01, respectively. \dot{V}_1/\dot{V}_2 is the volumetric flow rate ratio of the two fluids. Figure 2 shows the effects gravity and size (for a given $|\rho_1 - \rho_2|$ and σ), presented in the form of Eo ($\delta_{in}/W = 0.3$ and $Ca = 0.1$). As seen in Fig. 2, the interface evolution is not affected by gravity as long as $Eo \leq 1$. As the Eotvos number Eo decreases with the channel size, the effects of gravity becomes less important in the microchannels. Also notice that the development length increases as the channel becomes smaller (smaller Eotvos number Eo). A maximum development length is observed. Once this length is reached, further decrease in Eotvos number Eo does not alter the development length. Because the solutions are invariant for $Eo < 1$, Eo is set to 0 for the remainder of this Note. As a result, the development lengths are the maximum possible lengths.

Figure 3a shows the evolutions of both the interface and the velocity field along the flow direction, up to $x/W = 1$, where changes are significant. The interface and the velocity profiles of the present LSET solution agree well with that of the VOF. Figure 3b shows the pressure distribution across the flow direction. For a comparison to be made, the pressure field at a given axial location is adjusted by adding a constant so that the pressure at the lower plate is zero. Therefore, the axial pressure gradient $\partial p / \partial x$ cannot be inferred from Fig. 3. The pressure jump across the interface is obvious. However, the jump is not abrupt. In the CSF formulation, the surface tension force acts within a finite thickness of 2ϵ around the interface. The pressure varies smoothly across this interfacial thickness. Nevertheless, the magnitude of the pressure jump across the interface remains unaltered and is captured correctly. The pressure jump is larger in the developing region due to the larger curvature. The pressure jump reduces gradually as the curvature decreases along the flow direc-

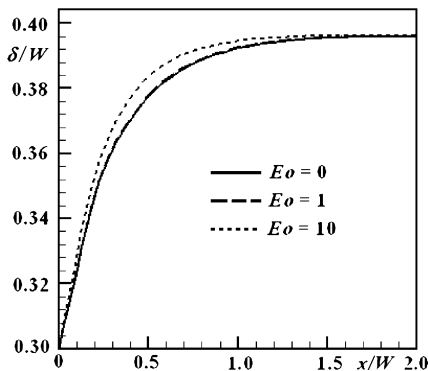


Fig. 2 Effect of Eo on interface evolution for $Re = 0.01$ and $Ca = 0.1$.

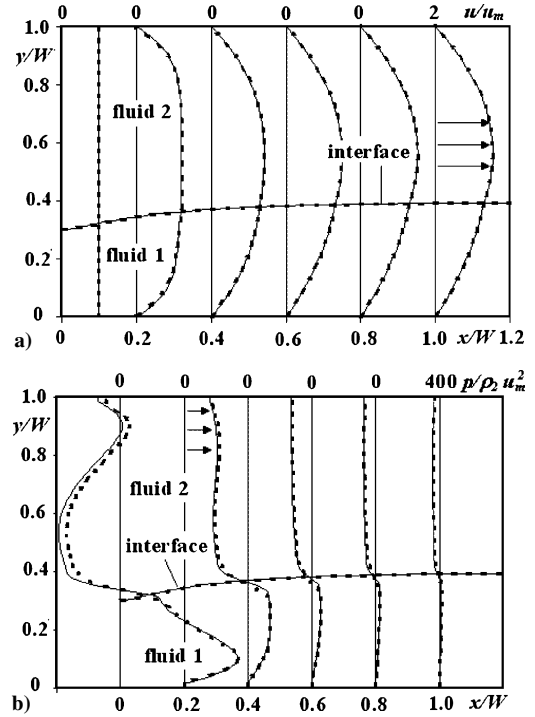


Fig. 3 Comparison between LSET and VOF: a) interface evolution and velocity profile along the flow direction and b) pressure distribution across the flow direction: ---, VOF and — LSET.

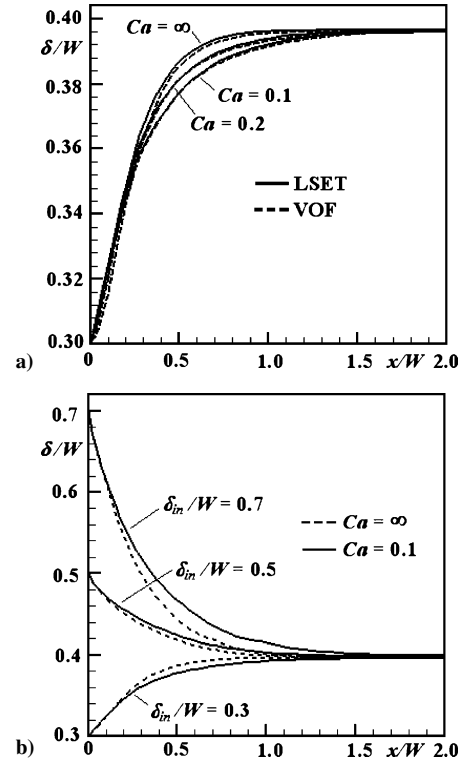


Fig. 4 For $Re = 0.01$ and $Eo = 0$, a) interface evolution for different Ca and b) interface evolution for different δ_{in}/W .

tion. Comparison is made with the pressure field predicted by VOF. There is good agreement between the two predictions except at $x/W = 0.2$. At this section, although both predict a similar trend, the pressure distribution is quantitatively different. The maximum error $(p_{VOF} - p_{LSET}) / (p_{max} - p_{min})$, with all values at $x/W = 0.2$, is around 6%.

The effect of surface tension on the interface evolution is shown in Fig. 4. Figure 4a shows that the interfaces predicted by the

present approach are in good agreement with that of the VOF (with $\delta_{in}/W = 0.3$). Once fully developed flow is attained, the interface converges to the same location irrespective of Ca . As the boundary layer develops in the inlet region, curvature of the interface is created. This nonzero interface curvature leads to a surface tension force that tends to flatten the interface. This, in turn, hinders the development of the boundary layer. Therefore, the entry length increases for smaller Ca flow where the surface tension force is larger.

For flow without surface tension, the fully developed velocity profiles and δ_E/W are functions of μ_1/μ_2 and \dot{V}_1/\dot{V}_2 and independent of δ_{in}/W (Refs. 5, 7, and 8). This is still valid for the case with surface tension because surface tension only affects the flow characteristics in the developing region. For demonstration, δ_{in}/W is varied while fixing \dot{V}_1/\dot{V}_2 and μ_1/μ_2 to $\frac{3}{7}$ and 2.0, respectively. The inlet velocities of both fluids have to be modified accordingly to maintain the same \dot{V}_1/\dot{V}_2 for different δ_{in}/W . Figure 4b shows the evolutions of the interface for $\delta_{in}/W = 0.3, 0.5$, and 0.7 , respectively, with and without surface tension. Although the interface locations at the inlet are different, all of the fully developed interfaces converge to the same location irrespective of the presence of surface tension. Again, the entry length increases with the presence of surface tension.

IV. Conclusions

The effect of surface tension on a stratified two-phase flow between parallel plates is investigated using the LSET method with a recently proposed LMC scheme. The surface tension term is modeled using the CSF model. The results from the present Note agree well with the results obtained using the VOF method. It is found that

surface tension effect is confined to the developing region where the interface curvature is nonzero. The entry length increases with the coefficient of surface tension. However, the interface location and velocity profile in the fully developed region are independent of surface tension.

References

- ¹Osher, S., and Sethian, J. A., "Fronts Propagating with Curvature-Dependent Speed: Algorithms Based on Hamilton–Jacobi Formulations," *Journal of Computational Physics*, Vol. 79, No. 1, 1988, pp. 12–49.
- ²Hirt, C. W., and Nichols, B. D., "Volume of Fluid (VOF) Methods for the Dynamics of Free Boundaries," *Journal of Computational Physics*, Vol. 39, No. 1, 1981, pp. 201–225.
- ³Unverdi, S. O., and Tryggvason, G., "A Front-Tracking Method for Viscous, Incompressible, Multi-fluid Flows," *Journal of Computational Physics*, Vol. 100, No. 1, 1992, pp. 25–37.
- ⁴Brackbill, J. U., Kothe, D. B., and Zemach, C., "A Continuum Method for Modelling Surface Tension," *Journal of Computational Physics*, Vol. 100, No. 2, 1992, pp. 335–354.
- ⁵Yap, Y. F., Chai, J. C., Toh, K. C., Wong, T. N., and Lam, Y. C., "Numerical Modeling of Unidirectional Stratified Flow With and Without Phase Change," *International Journal of Heat Mass Transfer*, Vol. 48, No. 3–4, 2005, pp. 477–486.
- ⁶Chang, Y. C., Hou, T. Y., Merriman, B., and Osher, S., "A Level Set Formulation of Eulerian Interface Capturing Methods for Incompressible Fluid Flows," *Journal of Computational Physics*, Vol. 124, No. 2, 1996, pp. 449–464.
- ⁷Bird, R. B., Stewart, W. E., and Lightfoot, E. N., *Transport Phenomena*, Wiley, New York, 1971, Chap. 2.
- ⁸Churchill, S. W., *Viscous Flows: The Practical Use of Theory*, Butterworths, Stoneham, MA, 1988, Chap. 3.